

5-1-2020

## Novel Automated Drill Apparatus for Accessing Equine Hoof Wall

Wellesley Dittmar  
*Mississippi State University*

Follow this and additional works at: <https://scholarsjunction.msstate.edu/honorsthesis>

---

### Recommended Citation

Dittmar, Wellesley, "Novel Automated Drill Apparatus for Accessing Equine Hoof Wall" (2020). *Honors Theses*. 74.

<https://scholarsjunction.msstate.edu/honorsthesis/74>

This Honors Thesis is brought to you for free and open access by the Undergraduate Research at Scholars Junction. It has been accepted for inclusion in Honors Theses by an authorized administrator of Scholars Junction. For more information, please contact [scholcomm@msstate.libanswers.com](mailto:scholcomm@msstate.libanswers.com).

Novel Automated Drill Apparatus for Accessing Equine Hoof Wall

By

Wellesley Dittmar

A Thesis

Submitted to the Faculty of

Mississippi State University

in Partial Fulfillment of the Requirements

for the Provost Scholarship

Mississippi State, Mississippi

April 2020

Copyright by  
Wellesley Dittmar  
2020

## ACKNOWLEDGEMENTS

The author would like to thank Dr. Filip To for overseeing and assisting in construction and testing of the device.

The author would also like to thank her parents for their continued support and financial contributions.

Finally, the author thanks the committee for their comments on this thesis.

## TABLE OF CONTENTS

ACKNOWLEDGEMENTS	i
CHAPTER	
1. INTRODUCTION	1
1.1 Motivation	1
1.2 Project Overview	1
2. THEORY AND BACKGROUND	2
3. MATERIALS AND METHODS	7
3.1 Device Materials	7
3.2 Software	17
3.3 Depth Measurement Methods	19
3.4 Statistical Methods	20
4. RESULTS	23
4.1 Preliminary Results	23
4.2 Statistical Analysis	23
5. CONCLUSION	24
5.1 Summary	24
5.2 Future Work	24
APPENDIX	25
REFERENCES	26

# CHAPTER 1

## INTRODUCTION

### **1.1 Motivation**

Equine laminitis is a common disease that causes lameness and death within the majority of afflicted horses. These deaths represent an extreme loss of capital for horse owners and professionals within the equine industry. Laminitis causes the bone within the equine hoof capsule to detach from the outer hoof wall and rotate downwards, placing extreme pressure upon the sole of the hoof and causing the animal immense pain. If detected in a timely manner, the effects of laminitis can be minimized or reversed to a limited degree; however, detection is complicated by the thick keratin layer of the outer hoof wall. This project seeks to create a window into that thick layer for safe monitoring of inner hoof conditions, allowing for early detection of laminitis warning signs, and possibly intervention or treatment.

### **1.2 Project Overview**

This project will create a novel automated scaffold system to allow for easy, accurate access hole creation in the keratin hoof layer. By using a combination of 3-dimensionally articulated scaffold pieces and a programmed motor, a rotating cutter can be placed in any location on the hoof capsule and can automatically create an access port of a desired depth within the hoof wall. Scaffold pieces will be manufactured within the Mississippi State University Department of Agricultural and Biological Engineering building and the motor will be programmed using university software tools. The device's efficiency will be tested by creating access ports in the hoof wall of a model equine foot. The depths of these ports will be measured and compared to the desired depths and statistical analysis will be performed.

## CHAPTER 2

### THEORY AND BACKGROUND

Laminitis is a common condition of hooved animals, with research on the disease dating back to the 1940s (Patterson-Kane et al., 2018). The disease is hallmarked by the failure of the attachment between the distal phalanx, commonly referred to as the pedal bone, and the outer keratinized hoof wall, the angled plane between the horse's ankle and where the hoof intersects the ground (Pollitt, 2004). This attachment is known as the lamellae and is comprised of specialized lamellar cells that bind the bone to the hoof wall (Pollitt, 2004). During the onset of laminitis, these lamellar cells stretch and deform, and the binding between individual cells as well as between cells and the hoof wall detaches (van Eps and Burns, 2019). Upon failure of this attachment, the pedal bone rotates downward and is continuously driven into the sole of the hoof by forces generated during locomotion (Pollitt, 2004). This bone movement crushes vasculature within the sole of the hoof and places immense pressure on the sole corium, causing incredible pain to the afflicted animal (Pollitt, 2004). Once a horse has contracted laminitis for the first time, its chances of relapsing increase dramatically, and 33% of all diagnosed cases must be humanely euthanized (Luthersson et al., 2017). Diagnosis of laminitis is incredibly difficult due to the thickness of the hoof wall, and signs do not appear until after damage has been done to hoof structures. This project aims to create a novel device to assist in detection before this threshold of damage is reached.

Clinical signs of laminitis are difficult to detect before irreversible damage to the hoof occurs. The most commonly noticed sign is sudden, acute lameness demonstrated during locomotion and a laminitic "stance" (Pollitt, 2004). This stance is characterized by the horse rocking back to place its body weight on its hind feet and alleviate pressure on the front hooves.

When viewed by radiographs, a characteristic displacement of the pedal bone is also visible (Pollitt, 2004). As the disease progresses, the hoof wall may deform to a noticeable degree and the sole of the hoof will flatten due to the constant pressure exerted by the rotating pedal bone (Pollitt, 2004). All of these signs indicate that the animal is in immense pain and, if not caught early enough, the damage is irreversible. If pain cannot be managed, humane euthanasia of the animal is often the recommended action.

There are three recognized phases in the progression of laminitis (Pollitt, 2004). The first phase is known as the developmental phase, which occurs before the horse displays any indication of pain. This phase occurs when there is a disturbance in an internal system of the equid. This disruption is thought to produce laminitic trigger molecules that contribute to later stages of the disease. Common causes of this developmental phase are hypothesized to include overfeeding, injury, and prolonged usage of corticosteroids (Pollitt, 2004). The second phase is referred to as the acute phase and is measured from the first indication of pain to the time when the pedal bone has first been determined to rotate via radiograph. In this phase, the lamellar cells are in the process of dying and pulling away from the hoof wall, so increased locomotion of the animal causes increased damage to these cells and worsens the microscopic damage (Pollitt, 2004). If discovered during this phase, the damage can possibly be reversed by applying ice to the affected hoof. The final phase, or chronic phase, results in permanent displacement of the pedal bone and symptoms such as hoof deformation, sole flattening, adoption of the characteristic stance, and chronic lameness (Pollitt, 2004). When this phase is reached, irreversible damage has been done to the hoof structures and the only treatments are pain management or euthanasia.

Three phenotypes of laminitis are recognized within the veterinary community (van Eps and Burns, 2019). The first phenotype is known as endocrinopathic laminitis and is hypothesized to be the most common form of the disease. Horses afflicted by equine metabolic syndrome (EMS) or pituitary pars intermedia dysfunction (PPID) are at higher risk for this phenotype due to their disrupted endocrine systems. The mechanisms by which the lamellar attachment fails in this phenotype are largely unknown, but recent studies have shown that lamellar cells have an affinity for insulin-like growth factor-1. This affinity indicates that an increase in insulin has a great impact in lamellar cells and can possibly alter their production of extracellular matrix. Therefore, an increase in insulin can disrupt the attachment between lamellar cells and cause their separation from the hoof wall, leading to laminitis.

The second phenotype of laminitis, sepsis-related laminitis, occurs as a response to systemic inflammation caused by bacterial infections (van Eps and Burns, 2019). Gram-negative bacteria and their byproducts are commonly implicated in this inflammatory response and can cause end-organ dysfunction as seen in septic humans. The inflammatory cytokines generated during this inflammation enter the lamellar tissue via the circulatory system, inducing conformational changes in the lamellar cells and disrupting their attachment to the hoof wall. Leukocyte migration has also been implicated in the development of this laminitis phenotype, but the exact mechanism remains unclear.

Supporting limb laminitis, the third phenotype, occurs upon injury to one leg of the equid. When only one front limb is injured, the loading on the opposing leg is increased dramatically (van Eps and Burns, 2019). This constant increase in loading is hypothesized to trigger lamellar remodeling, as well as disrupt the flow of blood through the loaded leg. The decrease in blood flow leads to glucose deprivation, triggering lamellar changes and inducing

onset of laminitis. All three phenotypes of laminitis often cross over and share common signs, as well as common progression pathways.

This project aims to create a novel apparatus to allow easy creation of access ports into the equine hoof wall. Once a protocol for safely entering the hoof wall has been developed, sensors or probes can be implanted in the hoof wall to detect changes in lamellar cells. These sensors can detect early onset of laminitis, allowing for treatment of the disease while the damage is still reversible. During the course of this project, a protocol to determine the thickness of an equine hoof wall from an x-ray image was developed and an automated drill apparatus was created. This apparatus was programmed with the hoof wall depth obtained from x-rays and was used to create an access port at the boundary between the hoof wall and the lamellar cells. This port can be used to sense hoof temperature, blood flow in the lamellar cells, and other cellular markers of the developmental phase of laminitis such as inflammatory cytokines or glucose. The development of this drill apparatus allows for early detection and treatment of this crippling disease, reducing the number of horses euthanized due to complications of laminitis.

This project sought to design an automated apparatus in order to accurately create access ports into a horse's hoof wall based on dimensions obtained from radiographs of the hoof. This access port will allow for placement of sensors and other diagnostic tools into the hoof wall to detect and directly treat laminitis. The created access ports can also be used to deliver drugs into the hoof wall to treat other common hoof ailments if necessary, before irreversible damage occurs.

The objectives associated with this design included:

1. Develop a set of definitive instructions by which a user can correctly measure the thickness of a horse hoof from an x-ray image of that hoof.
2. Develop a computer-user interface to allow the user to input this determined thickness into the drill, thereby defining the depth to which the drill must penetrate the hoof wall. This computer program must be able to perform the necessary computation to internally generate control instructions for the drill.
3. Design and develop a prototype apparatus to demonstrate the concept and functionalities of the drill upon a model hoof.

The capabilities and constraints defined for this project included:

1. A low-cost miniature or handheld drill must be incorporated as the means for creating an access hole.
2. The system apparatus must allow for user input of drilling depth.
3. The apparatus must also be able to work automatically in creating the access port desired.
4. The access hole must be within a certain percent of prescribed target depth.
5. There must be a verification of results using manual means.
6. The apparatus can only be demonstrated on cast hooves or cadaver hooves to prevent the use of animals in the design process.

CHAPTER 3  
MATERIALS AND METHODS

**3.1 Device Materials**

**Base**

The base of the apparatus consists of a plywood square, 24 inches in length and width and 0.75 inches thick. Figure 1 details the dimensions of the base platform. Two 0.31-inch bolt holes are drilled through the base at one side to allow for removable connection to the hinge pieces. Two pieces of 0.25-inch plywood are placed underneath the base to allow clearance for the connecting bolts. The purpose of this base is to provide a flat, uniform surface for a horse to support its hoof upon while drilling occurs.

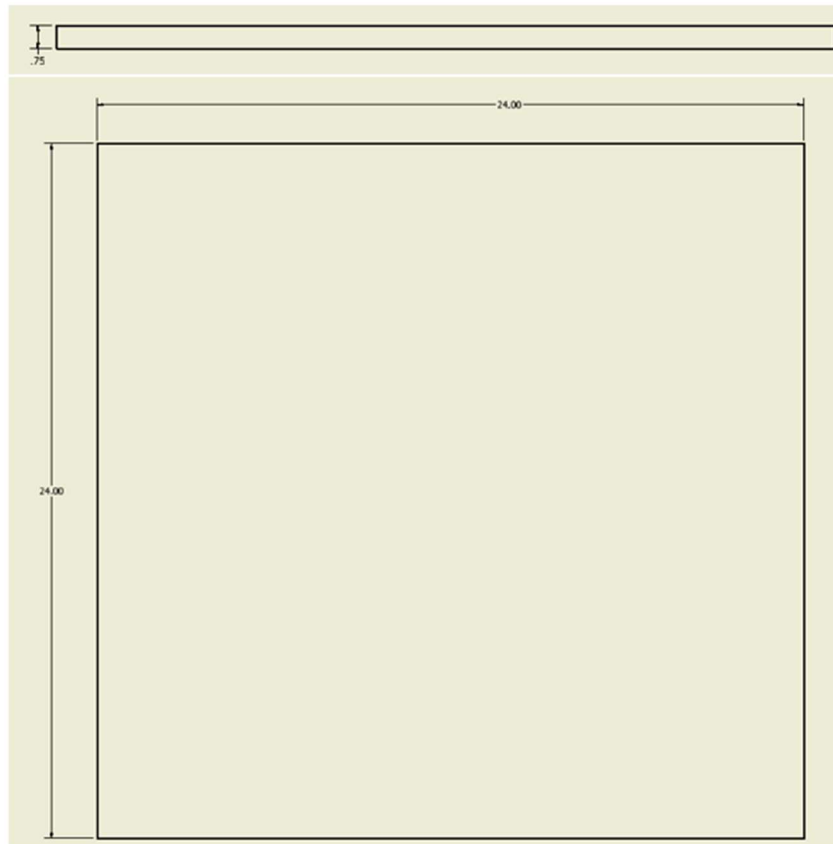


**Figure 1.** Base platform

## Hinge

A three-dimensional hinging system allows the drill apparatus to move over 100 degrees in all directions. Figure 2 depicts hinge part 1. This system consists of two interlocking plywood pieces denoted as hinge part 1 and hinge part 2. Hinge part 1 is 6.5 inches tall, 5 inches long, and 3.75 inches wide. There is a 3.5-inch-deep, 0.8-inch-wide groove in the center of the piece to allow for connection to hinge part 2. A 0.31-inch bolt hole crosses the central groove, and a 0.5-inch long, 0.375-inch-tall slot accommodates a nut to connect hinge part 1 to the base platform. This piece was constructed by gluing multiple carvings together.

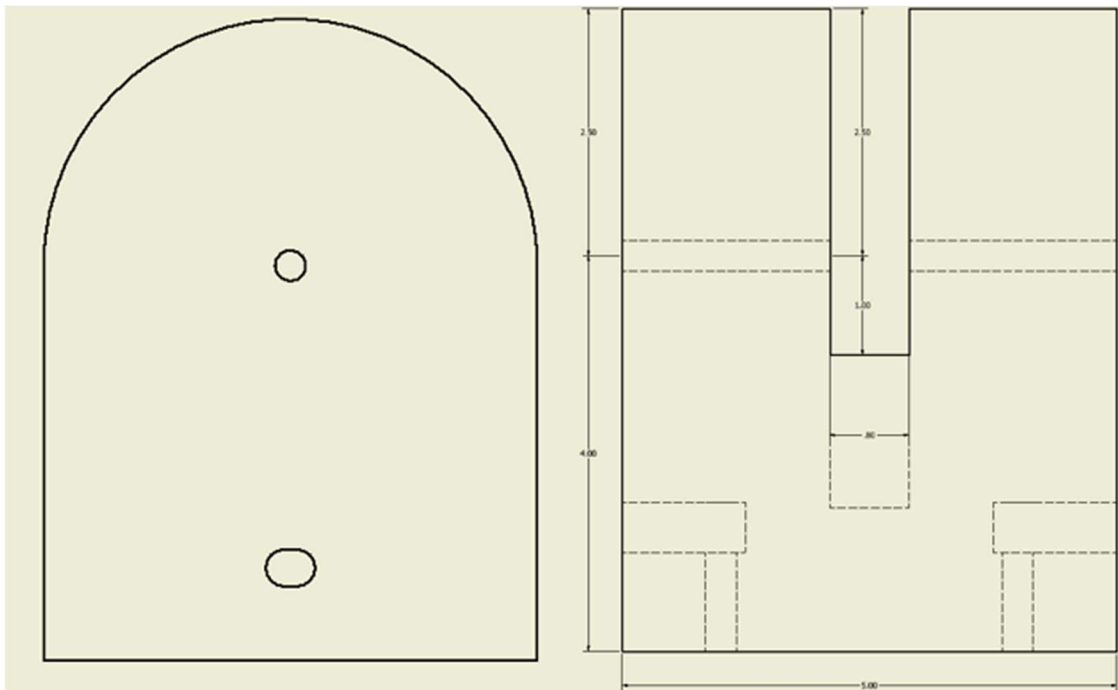


**Figure 2.** Hinge part 1

Figure 3 shows hinge part 2. Hinge part 2 is 13 inches tall, 5 inches long, and 3.75 inches wide. A 6.5-inch-long 0.75-inch-wide protrusion extends from the 6.5-inch-long top and fits into the groove in hinge part 1 and is connected with a 0.31-inch bolt hole. At the top of the piece, a

3.5-inch-deep, 0.8-inch-wide groove allows for connection to the backboard via a 0.31-inch bolt hole.

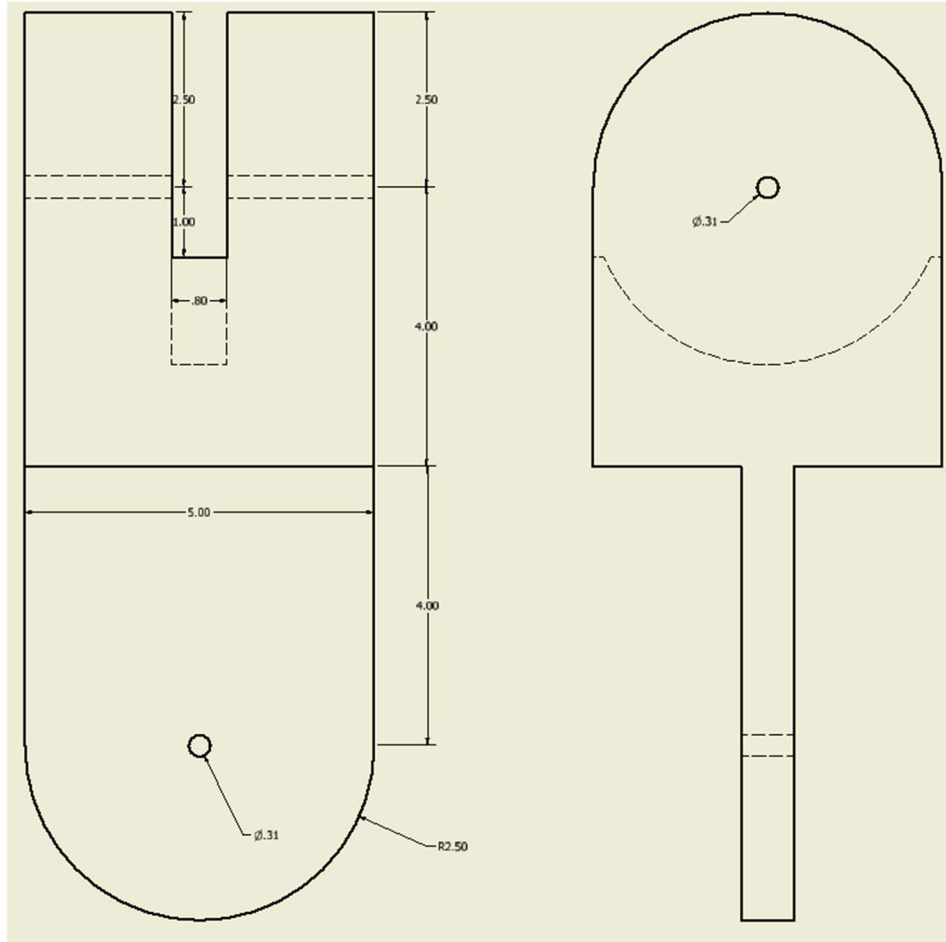


**Figure 3.** Hinge part 2

### **Backboard**

The plywood backboard connects to hinge part 2 and supports the drill stage. This component is 18.5 inches tall, 5 inches long, and 0.75 inches wide. The bottom consists of a 2.5-inch-long, 0.75-inch wide circle that fits into the groove of hinge part 2 and is connected by a 0.31-inch bolt hole. 3 pairs of 0.31-inch bolt holes are located at various distances along the backboard, corresponding to the locations of the bolt holes in the drill stage. This allows the drill stage to connect to the backboard. This piece is shown in Figure 4.

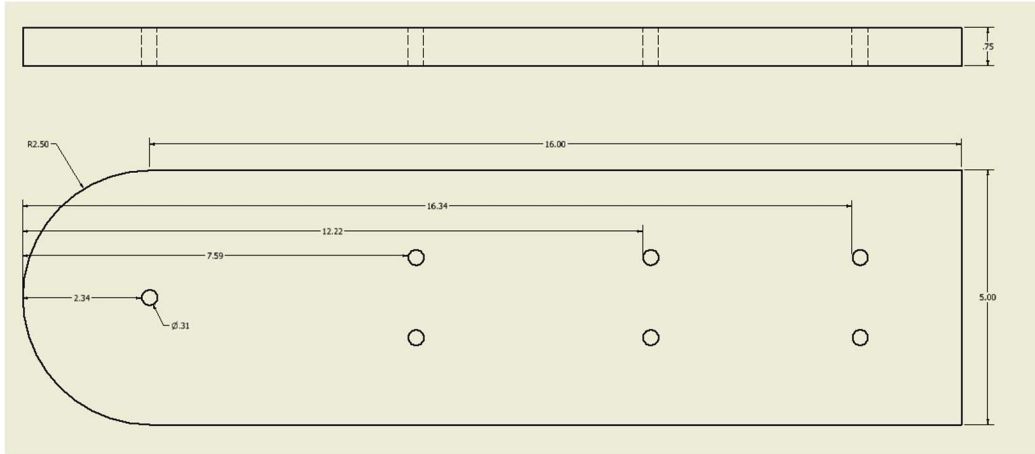


**Figure 4.** Backboard

### Linear Actuator

Figure 5 depicts the drill stage. A 300-millimeter Linear Rail Slide Cross SFU1605 Ballscrew Module C7 drill stage connects to the backboard and allows the drill to slide along a vertical axis. The stage is also connected to the motor, which allows automated movement of the drill along the stage. This drill stage is 18 inches long and 3 inches wide and connects to the backboard via 6 sets of bolt holes.

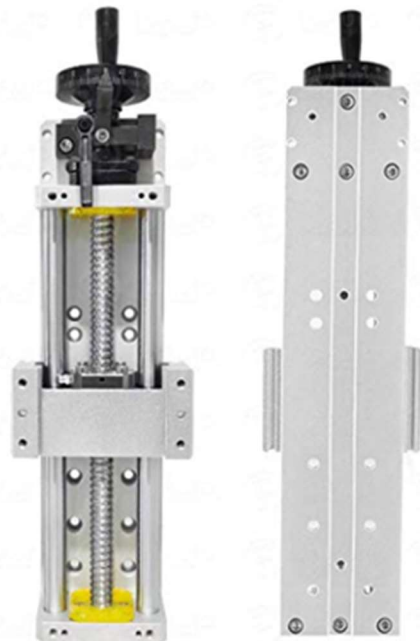


**Figure 5.** Linear actuator (stage) (*Updated CNC Manual Sliding Table*, n.d.)



The motor is connected to the drill stage via two 3D-printed adaptors, each of which are 1 inch tall and 0.8 inches wide. Two slots in the side allow for placement of two heat set inserts in each adaptor. One side of the adaptor is sized to connect to the motor shaft (0.11 inches). In the stage-to-motor coupling, the other side is sized to connect to the drill stage column (0.21 inches); in the motor-to-hand wheel coupling, the other side is sized to connect to the hand crank of the drill stage (0.39 inches). Figure 8 shows the stage-to-motor coupling and Figure 9 shows the motor-to-hand wheel coupling. The motor is mounted to the linear actuator stage via a motor bracket, which is shown in Figure 10.

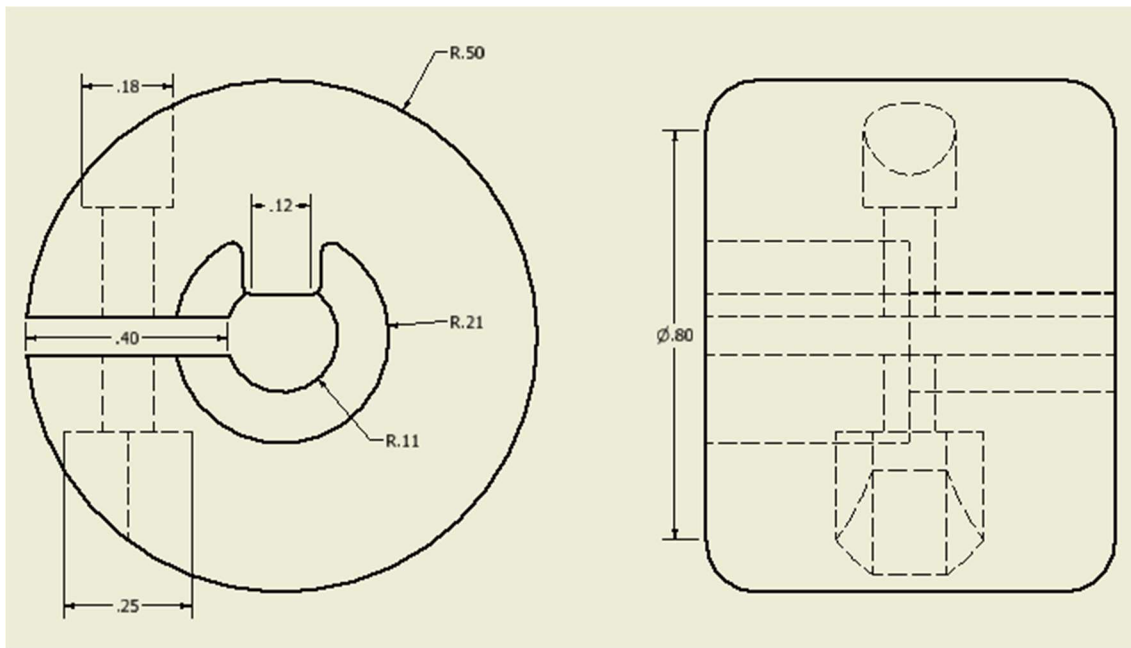


**Figure 8.** Stage-to-motor coupling

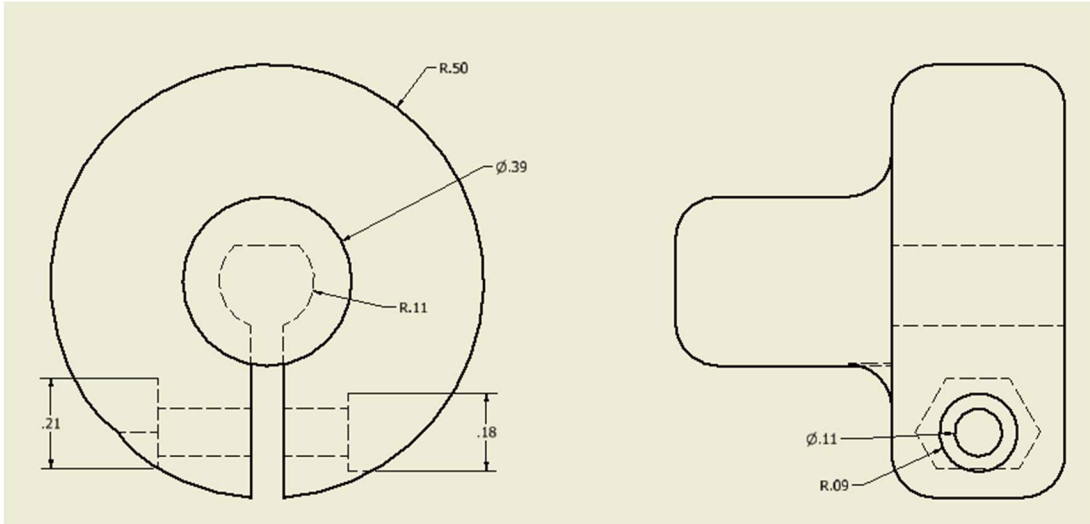


**Figure 9.** Motor shaft-to-hand wheel coupling

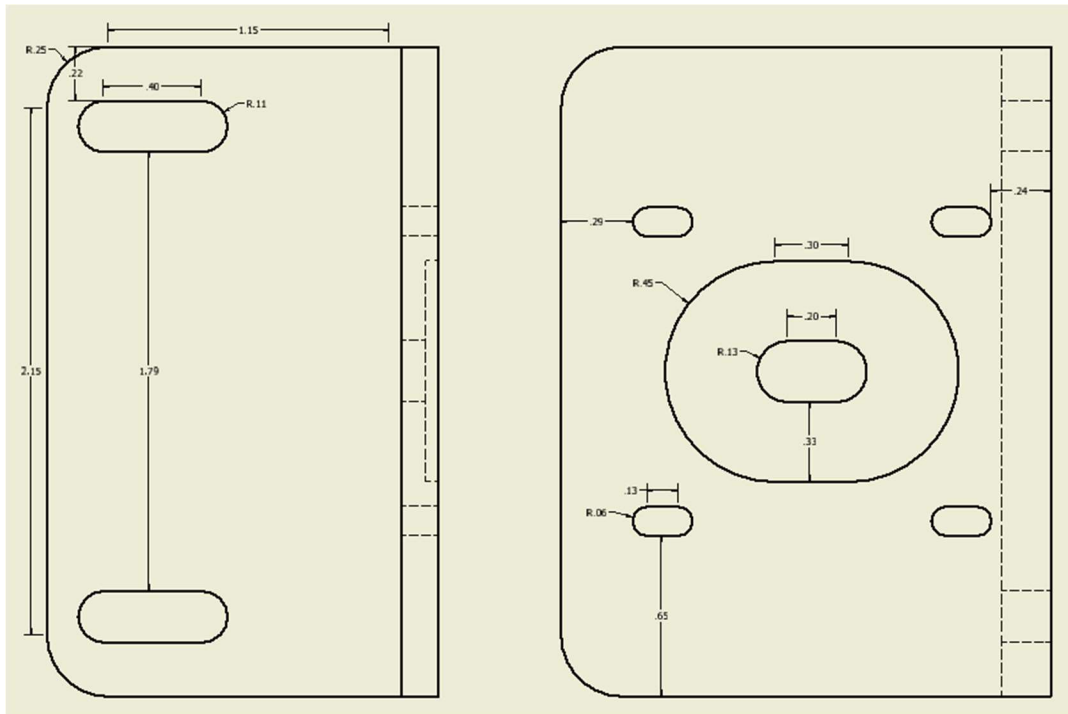


**Figure 10.** Motor mounting plate

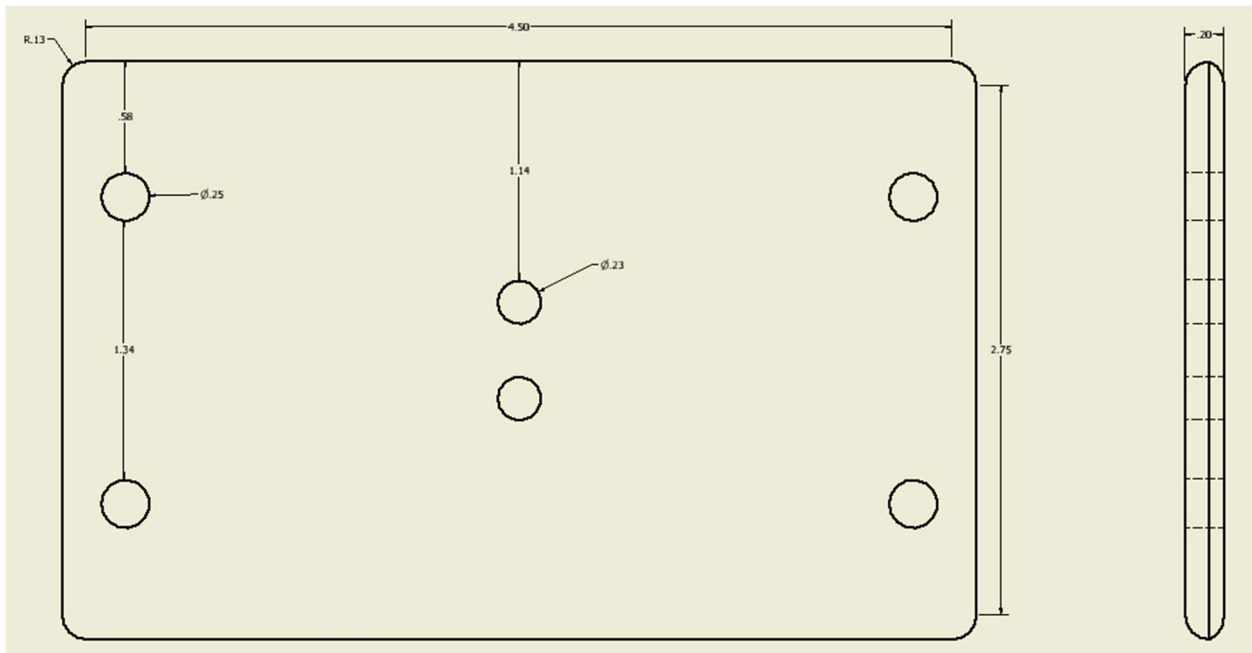
## Drill

Figure 11 depicts the drill. A Goxawee Rotary electric drill is connected to the drill stage and creates the access port within the hoof wall. This drill comes with a variety of drill bits to allow for varying port size and shape and is easily plugged into a standard wall outlet for power.



**Figure 11.** Drill (*GOXAWEE Rotary Tool Kit, n.d.*)

The drill is connected to the drill stage by a clamp and a mounting plate. The mounting plate is bolted to the drill stage using two 0.23-inch bolts and four 0.25-inch bolts. It is 5 inches long, 3 inches tall, and 0.2 inches thick. Figure 12 depicts the clamp mounting plate.



**Figure 12.** Clamp mounting plate

The clamp itself is 5 inches long and 3 inches tall. It has two arms surrounding a 1.96-inch circle to hold the drill. The arms have a flat, 0.75-inch extension after the circle with a 0.14-inch bolt hole and 0.4-inch nut socket to allow for closure of the clamp. There is a 0.35-inch recess behind the circular drill socket to allow for two 0.25-inch bolts to connect the clamp to its backboard. Figure 13 depicts the clamp.

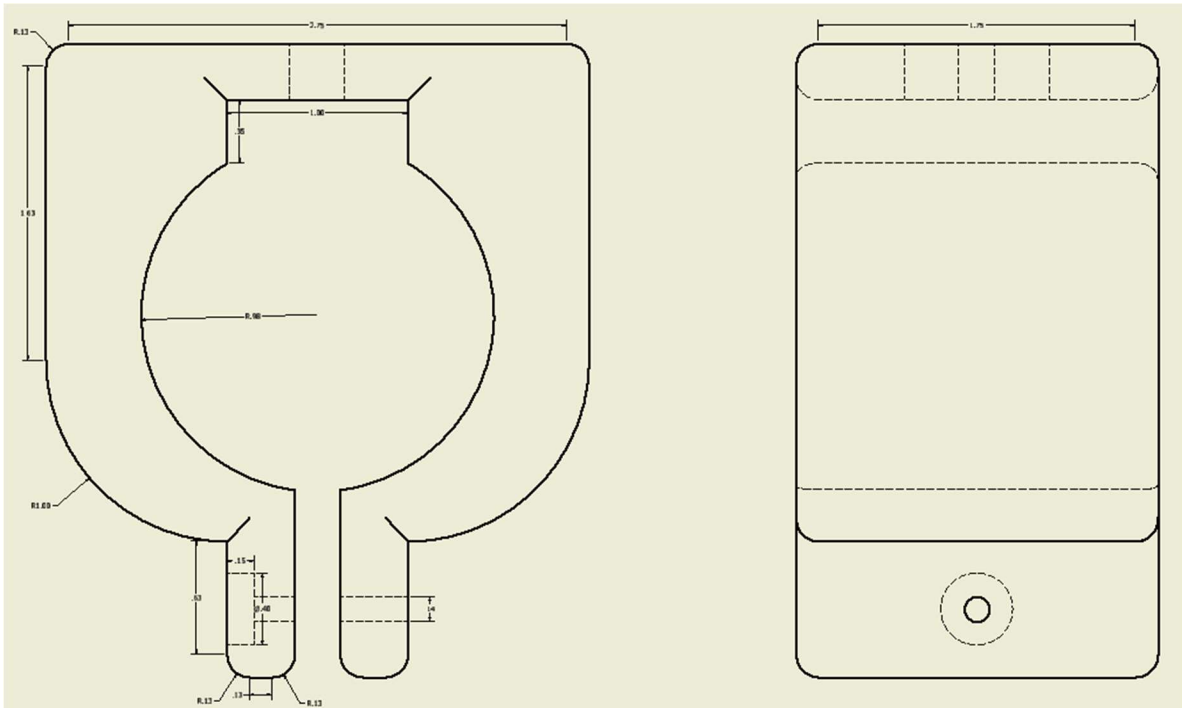


**Figure 13.** Clamp – Top View and Side View

### **Final Assembly of Framework**

The final assembly is constructed of the previously detailed pieces. Its total height is 35.5 inches. All pieces are connected by 0.25-inch bolts and the corresponding nuts. The motor and drill connect to a standard electrical outlet via power cords. Figure 14 demonstrates the rough scaffold of the entire assembly.



**Figure 14.** Final assembly scaffold

### Electrical Components

The following block diagram illustrates the electrical connectivity between components of the apparatus:

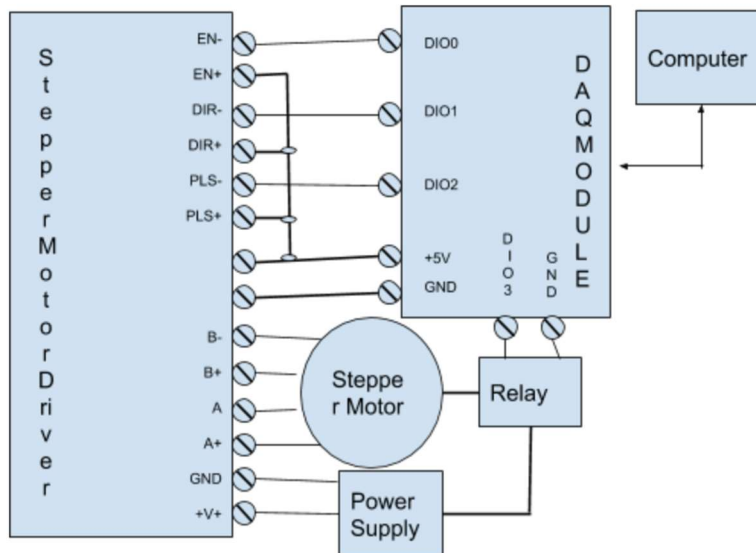


**Figure 15.** Block diagram of the electrical components of the apparatus

The stepper motor, which actuates the stage is driven by the Stepper Motor Driver, and the control signals to the Stepper Motor Driver are generated by a myDAQ control module (National Instruments myDAQ). The myDAQ is connected to a computer via a USB cable. Figure 16 shows the picture of the completed system including the electrical interconnections.

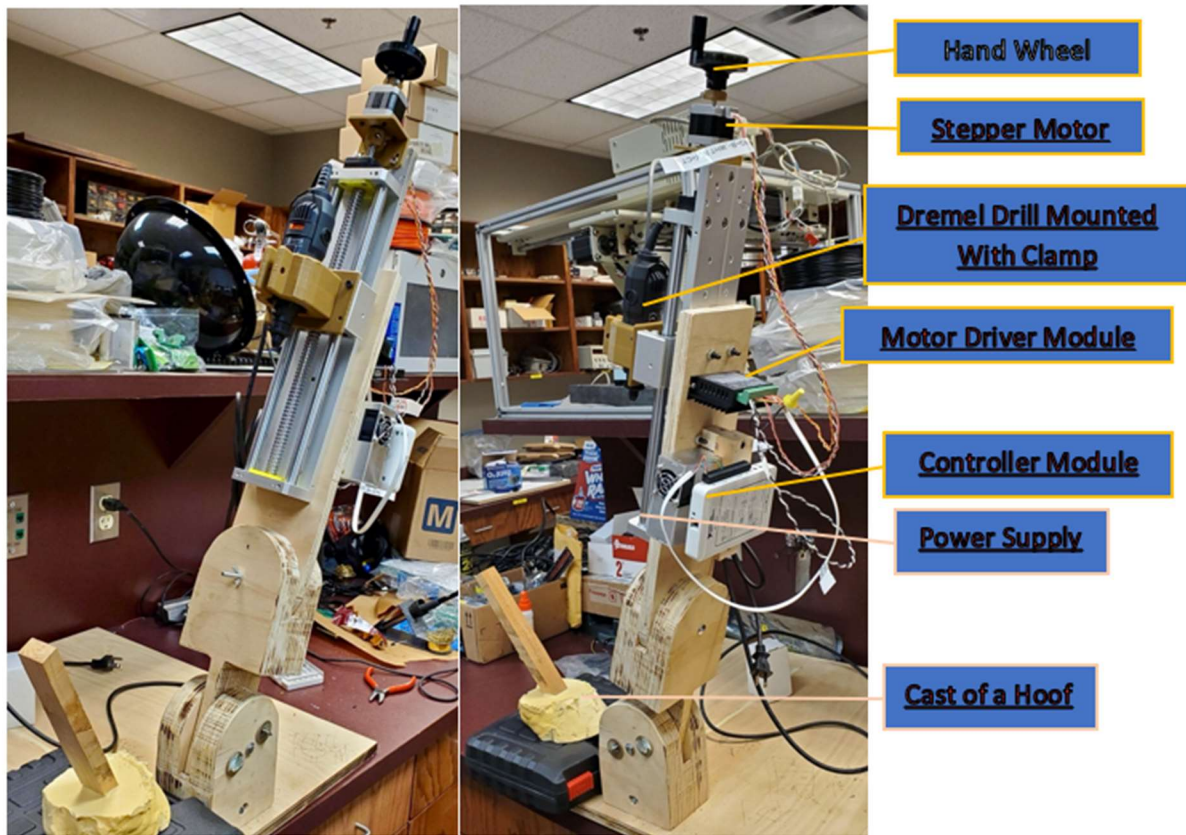


**Figure 16.** Finished apparatus

### 3.2 Software

The software developed to control the apparatus was written in LabVIEW (National Instruments), the graphical user interface of which is shown in Figure 17.

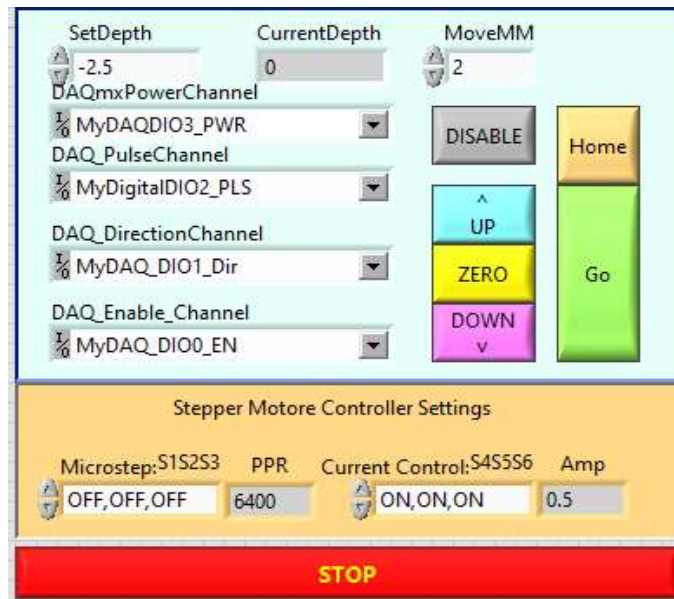


**Figure 17.** User interface

The tasks implemented in the software include motion and calibration. The motion category of the tasks includes the ZERO button, which sets the current position of the stage as the “zero” location of the apparatus; and the UP and DOWN buttons for changing the stage position up or down relative to the zero position. The distance the stage is moved by the UP and DOWN buttons is determined by a numeric value specified by the MoveMM parameter. In order to allow for manual positioning of the stage (using the hand wheel), the motor controller can be disabled by pressing the DISABLE button; a HOME button is incorporated to allow the stage to be repositioned back to “zero”. To execute the drilling operation, a GO button automatically activates the drill and creates the access hole according to the numeric setting of the desired depth in the SetDepth box.

A typical method of using the system is as follows:

1. The user uses the hand wheel to position the stage so that the drill bit touches the exterior wall of the hoof, then presses ZERO to set this location as the “zero” position.

2. The user specifies the desired depth of the access port in millimeters (in 0.1 mm resolution).
3. The user presses GO, after which the system will power the drill, create the hole, and retract the stage after the operation is completed.
4. If a repeated operation is needed, the user will disable the motor by pressing the DISABLE button and then repeat the operation described in steps 1 to 3.

### **3.3 Depth Measurement Methods**

To test the accuracy of the motor's programming and ensure that the drill bit does not enter past a desired depth, the drill apparatus would have been adjusted until the drill stage lays horizontal to the ground. The user would input several different depths into the motor controller and the distance the drill moves would be measured. This measured movement would be compared to the original, desired depth to determine the accuracy of the drill's motion. Each distance would be repeated 5 times and statistics will be run on each set of distances to determine the significance of the results. This testing would prove if the apparatus is safe for use on live tissue.

After the horizontal distance testing, the apparatus would be tested on a model hoof to explore its three-dimensional motion. The test hoof would be placed in a variety of locations upon the base platform and the apparatus would be maneuvered until the drill bit is perpendicular to the hoof face. The data generated from this testing would be qualitative, so no statistics will be run. Instead, this testing is designed to be a simulation of how placement of the apparatus would occur when used in the field. Figure 18 shows the model hoof used in this testing.



**Figure 18.** Model hoof

### **3.4 Statistical Methods**

In order to determine if the device is accurate enough for use on a live animal, statistical analysis of the distance results would have been performed. For each of the five distances measured while the drill stage was horizontally tested, a two-tailed, one-sample t-test would have been performed to compare the physical distance to the user-input distance. This test would have indicated if the mean distance traveled for each test input was greater or less than the desired distance.

To perform a two-tailed, one-sample t-test, the mean of each sample set would first be calculated by adding all measured distances together and dividing them by 5, the number of samples.

$$\underline{y} = \frac{y_1+y_2+y_3+y_4+y_5}{5} \quad \text{(Equation 1.)}$$

Equation 1 gives the mean of sample set, where  $\underline{y}$  is the mean,  $y_1$  to  $y_5$  are generated data points, and 5 is the sample size. After finding the mean, the sample standard deviation would be calculated. This is done by subtracting the mean from an input distance, squaring the result, and repeating this process for each input distance. These squared distances are added together and divided by the number of sample sizes minus 1. Finally, taking the square root of this number provides the standard deviation.

$$\sigma = \sqrt{\frac{(y_1 - \underline{y})^2 + (y_2 - \underline{y})^2 + (y_3 - \underline{y})^2 + (y_4 - \underline{y})^2 + (y_5 - \underline{y})^2}{5-1}} \quad \text{(Equation 2.)}$$

Equation 2 gives the standard deviation, where  $\sigma$  is the standard deviation,  $\underline{y}$  is the mean,  $y_1$  to  $y_5$  are generated data points, and 5 is the sample size. Lastly, a test statistic (t-value) would have been found using the standard deviation. The t-value can be calculated by subtracting the input value from the mean and dividing the result by the standard deviation over the square root of the sample size.

$$t = \frac{y - m_0}{\sigma/\sqrt{5}} \quad \text{(Equation 3.)}$$

Equation 3 shows the test statistic, where t is the t-value, where  $\underline{y}$  is the mean,  $m_0$  is the input distance,  $\sigma$  is the standard deviation, and 5 is the sample size. From these values, a p-value for each test input would have been calculated. This p-value represents the probability of statistical insignificance. Therefore, it would have indicated if the results generated from testing were statistically significant and able to be used as a predictor for future behavior of the device.

The p-value would have been generated using computer software, and a p-value of less than 0.05 would have been considered statistically significant.

## CHAPTER 4

### RESULTS

#### **4.1 Preliminary Results**

Due to the university closures and residence hall shutdowns occurring across the university, no testing was able to be done on this device. If testing had occurred, the motor would have been programmed to move 1 centimeter, 2 centimeters, 3 centimeters, 4 centimeters, and 5 centimeters. The physical distance that the drill bit moved would be measured with a pair of calipers. Each distance would be repeated five times, and a distance table would have been generated from this data.

#### **4.2 Statistical Analysis**

Since no data was generated from this device, no t-tests were able to be performed. If data was collected, test statistic values would have been calculated using Equations 1-3. P-values would have been generated for each t-value, and the results would have been evaluated for statistical significance. If the device was statistically significant at each input distance, it would have been considered safe for use at that distance on a live animal.

## CHAPTER 5

### CONCLUSION

#### **5.1 Summary**

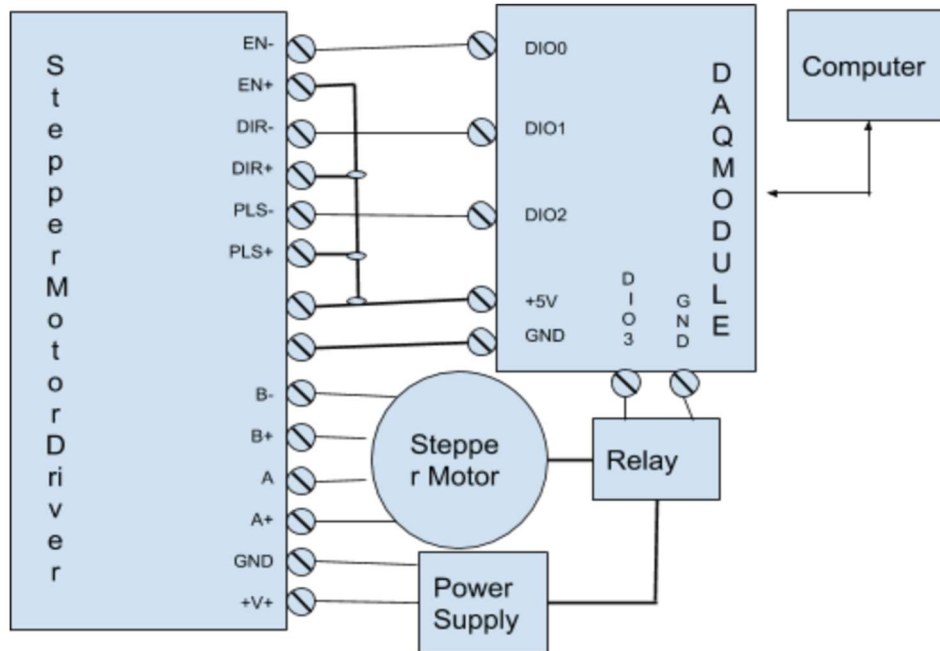
This project was intended to design a novel drill apparatus to allow for easy access to the equine hoof wall. Because the thick keratin layer of the outer equine hoof hinders detection of laminitis, access ports drilled into this layer could serve as a useful window into the interior of the foot. A three-dimensional hinging system and automated drill column would allow this device to be placed anywhere on the hoof with ease in order to precisely drill into the hoof face. Due to the COVID-19 outbreak in the United States at the time of this project, it was not able to be completed; however, the scaffold proves that the idea has merit and the device can be operated by hand when assembled correctly.

#### **5.2 Future Work**

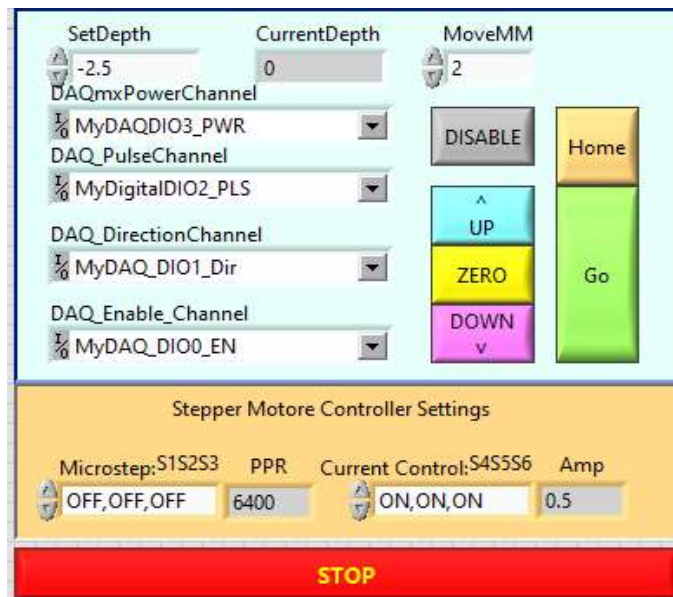
Suggestions for improvement include automating the motor to allow for finer control of drill bit placement and scaling the apparatus down to reduce weight and improve transportation ability.

In the future, novel sensors will be developed to fit within the created access ports. These sensors will monitor temperature and blood flow within the hoof capsule and detect early irregularities that hallmark progression of laminitis. These sensors will be semi-permanent and mounted to the hoof for an extended period of time to allow for long-term monitoring, which is ideal for animals known to be at high risk for disease development.

## APPENDIX



Wiring Diagram



LabVIEW Software User Interface and Block Diagram

## REFERENCES

- GOXAWEE Rotary Tool Kit with MultiPro Keyless Chuck and Flex Shaft – 140pcs Accessories Variable Speed Electric Drill Set for Crafting Projects and DIY Creations.* (n.d.). Amazon. Retrieved February 22, 2020 from [https://www.amazon.com/gp/product/B07FSBY9GV/ref=ppx\\_yo\\_dt\\_b\\_search\\_asin\\_title?ie=UTF8&psc=1](https://www.amazon.com/gp/product/B07FSBY9GV/ref=ppx_yo_dt_b_search_asin_title?ie=UTF8&psc=1).
- Luthersson, N., Mannfalk, M., Parkin, T.D. H., Harris, P. (2017). Laminitis: Risk Factors and Outcome in a Group of Danish Horses. *Journal of Equine Veterinary Science*, 53, 68-73. <https://doi.org/10.1016/j.jevs.2016.03.006>
- Patterson-Kane, J.C., Karikoski, N. P, McGowan, C. M. (2018). Paradigm shifts in understanding equine laminitis. *The Veterinary Journal*, 231, 33-40. <https://doi.org/10.1016/j.tvjl.2017.11.011>
- Pollitt, C. C. (2004). Equine laminitis. *Clinical Techniques in Equine Practice*, 3(1), 34-44. <https://doi.org/10.1053/j.ctep.2004.07.003>
- Stepper Motor Nema17, Unipolar, Dual Shaft, 40mm 34.1 Ncm 2A 6-Lead Hobby CNC 3D Printer.* (n.d.) Amazon. Retrieved February 22, 2020 from [https://www.amazon.com/Stepper-Nema17-Unipolar-34-1Ncm-Printer/dp/B06ZZ74KWN/ref=cm\\_cr\\_arp\\_d\\_product\\_top?ie=UTF8](https://www.amazon.com/Stepper-Nema17-Unipolar-34-1Ncm-Printer/dp/B06ZZ74KWN/ref=cm_cr_arp_d_product_top?ie=UTF8).
- Updated CNC Manual Sliding Table 300mm Linear Rail Slide Cross SFU1605 Ballscrew C7 Linear Stage Actuator DIY CNC Router Parts.* (n.d.). Amazon. Retrieved February 22, 2020 from [https://www.amazon.com/Updated-Sliding-SFU1605-Ballscrew-Actuator/dp/B081GTW49C/ref=sr\\_1\\_9?keywords=manual+sliding+table&qid=1582408342&sr=8-9](https://www.amazon.com/Updated-Sliding-SFU1605-Ballscrew-Actuator/dp/B081GTW49C/ref=sr_1_9?keywords=manual+sliding+table&qid=1582408342&sr=8-9).
- Usongshine Stepper Motor Driver TB6600 4A 9-42V Nema 17 Stepper Motor Driver CNC Controller Single Axes Phase Hybrid Stepper Motor for CNC/42 57 86 Stepper Motor.* (n.d.). Amazon. Retrieved February 22, 2020 from [https://www.amazon.com/UsongShine-Stepper-Controller-Arduino-Printer/dp/B07HHS14VQ/ref=sr\\_1\\_3?keywords=Usongshine%2BStepper%2BMotor%2BDriver%2BTB6600&qid=1582409064&sr=8-3&th=1#detail-bullets](https://www.amazon.com/UsongShine-Stepper-Controller-Arduino-Printer/dp/B07HHS14VQ/ref=sr_1_3?keywords=Usongshine%2BStepper%2BMotor%2BDriver%2BTB6600&qid=1582409064&sr=8-3&th=1#detail-bullets)
- van Eps, A. W., Burns, T. A. (2019). Are There Shared Mechanisms in the Pathophysiology of Different Clinical Forms of Laminitis and What are the Implications for Prevention and Treatment? *Veterinary Clinics of North America: Equine Practice*, 35(2), 379-398. <https://doi.org/10.1016/j.cveq.2019.04.001>